uni- and biparentally reared broods. Male dyads, therefore, had the same genetic parents, and the only difference between them was that one was raised under a uniparental regime and the other a biparental regime. Males had fresh food and water available throughout the experiment. Before being introduced to the mate choice apparatus, females were housed in a cage out of sight of the test males, so were unable to assess the choice of other females or make any previous assessment of either male. The order in which females were introduced to males was varied between each sibling pair. Trials were video-recorded by N.J.R. and watched by I.R.H., who was unaware of the identity of the test males. Females were recorded as making a preference for the male on the side of the cage at which she spent most of her time during the test. The experiment was conducted under the required conditions of ultraviolet (full spectrum) lighting[26].

Statistical analysis

We analysed the data using SPSS for Windows 10.0 and S-Plus 2000. We tested all data for normality and homogeneity of variances before analysis. All tests are two-tailed.

Received 28 September 2001; accepted 21 January 2002.

1. Clutton-Brock, T. H. *The Evolution of Parental Care* (Princeton Univ. Press, New Jersey, 1991).
2. Trivers, R. L. in *Sexual Selection and the Descent of Man* (ed. Campbell, B.) 136–179 (Aldine, Chicago, 1972).
3. Parker, G. A. Models of parent–offspring conflict .V. Effects of the behaviour of the two parents. *Anim. Behav.* **33,** 519–533 (1985).
4. Westneat, D. F. & Sargent, R. C. Sex and parenting: the effects of sexual conflict and parentage on parental strategies. *Trends Ecol. Evol.* **11,** 87–91 (1996).
5. McNamara, J. M., Houston, A. I., Barta, Z. & Osorno, J.-L. Should young ever be better off with one parent than with two? *Behav. Ecol.* (in the press).
6. Hurst, L. D., Atlan, A. & Bengtsson, B. O. Genetic conflicts. *Q. Rev. Biol.* **71,** 317–364 (1996).
7. Godfray, H. C. J. in *Levels of Selection in Evolution* (ed. Keller, L.) 100–120 (Princeton Univ. Press, New Jersey, 1999).
8. Lessells, C. M. in *Levels of Selection in Evolution* (ed. Keller, L.) 75–99 (Princeton Univ. Press, New Jersey, 1999).
9. Pomiankowski, A. in *Levels of Selection in Evolution* (ed. Keller, L.) 121–152 (Princeton Univ. Press, New Jersey, 1999).
10. Chapman, T. & Partridge, L. Sexual conflict as fuel for evolution. *Nature* **381,** 189–190 (1996).
11. Parker, G. A. & Partridge, L. Sexual conflict and speciation. *Phil. Trans. R. Soc. Lond. B* **353,** 261–274 (1998).
12. Smith, H. G. & Härdling, R. Clutch size evolution under sexual conflict enhances the stability of mating systems. *Proc. R. Soc. Lond. B* **267,** 2163–2170 (2000).
13. Rice, W. R. Sexually antagonistic male adaptation triggered by experimental arrest of female evolution. *Nature* **381,** 232–234 (1996).
14. Stockley, P. Sexual conflict resulting from adaptations to sperm competition. *Trends Ecol. Evol.* **12,** 154–159 (1997).
15. Birkhead, T. R. & Møller, A. P. (eds) *Sperm Competition and Sexual Selection*: (Academic, New York, 1998).
16. Gavrilets, S. Rapid evolution of reproductive barriers driven by sexual conflict. *Nature* **403,** 886–889 (2000).
17. Moore, A. J., Gowaty, P. A., Wallin, W. G. & Moore, P. J. Sexual conflict and the evolution of female mate choice and male social dominance. *Proc. R. Soc. Lond. B* **268,** 517–523 (2000).
18. Partridge, L. & Hurst, L. D. Sex and conflict. *Science* **281,** 2003–2008 (1998).
19. Sasvári, L. Reproductive effort of widowed birds. *J. Anim. Ecol.* **55,** 553–564 (1986).
20. Bart, J. & Tornes, A. Importance of monogamous male birds in determining reproductive success. *Behav. Ecol. Sociobiol.* **24,** 109–116 (1989).
21. Wolf, L., Ketterson, E. D. & Nolan, V. Behavioural response of female dark-eyed juncos to experimental removal of their mates: implications for the evolution of parental care. *Anim. Behav.* **39,** 125–134 (1990).
22. Whittingham, L. A., Dunn, P. O. & Robertson, R. J. Female response to reduced male parental care in birds: an experiment in tree swallows. *Ethology* **96,** 260–269 (1994).
23. Markman, S., YomTov, Y. & Wright, J. The effect of male removal on female parental care in the orange-tufted sunbird. *Anim. Behav.* **52,** 437–444 (1996).
24. Mock, D. W. & Parker, G. A. *The Evolution of Sibling Rivalry* (Oxford Univ. Press, Oxford, 1997).
25. Lessells, C. M. Parentally-biased favouritism: why should parents specialize in caring for different offspring? *Phil. Trans. R. Soc. Lond. B* (in the press).
26. Bennett, A. T. D., Cuthill, I. C., Partridge, J. C. & Maier, E. J. Ultraviolet vision and mate choice in zebra finches. *Nature* **380,** 433–435 (1996).
27. Smith, C. C. & Fretwell, S. D. The optimal balance between size and number of offspring. *Am. Nat.* **108,** 499–506 (1974).
28. Chase, I. D. Cooperative and non-cooperative behaviour in animals. *Am. Nat.* **115,** 827–857 (1980).
29. Houston, A. I. & Davies, N. B. in *Behavioural Ecology* (eds Sibley, R. M. & Smith, R. H.) 471–487 (Blackwell Scientific, Oxford, 1985).
30. McNamara, J. M., Gasson, C. E. & Houston, A. I. Incorporating rules for responding into evolutionary games. *Nature* **401,** 368–371 (1999).

Acknowledgements

We thank I. P. F. Owens, L. S. Forbes, C. M. Lessells and J. M. McNamara for comments on the manuscript. The project was funded by the Natural Environment Research Council.

Competing interests statement

The authors declare that they have no competing financial interests.

Correspondence and requests for materials should be addressed to I.R.H. (e-mail: i.hartley@lancaster.ac.uk).

Direct cortical input modulates plasticity and spiking in CA1 pyramidal neurons

Miguel Remondes & Erin M. Schuman

Caltech/Howard Hughes Medical Institute, Division of Biology, 216-76, Pasadena, California 91125, USA

The hippocampus is necessary for the acquisition and retrieval of declarative memories[1,2]. The best-characterized sensory input to the hippocampus is the perforant path projection from layer II of entorhinal cortex (EC) to the dentate gyrus[3,4]. Signals are then processed sequentially in the hippocampal CA fields before returning to the cortex via CA1 pyramidal neuron spikes. There is another EC input—the temporoammonic (TA) pathway—consisting of axons from layer III EC neurons that make synaptic contacts on the distal dendrites of CA1 neurons[3,5,6]. Here we show that this pathway modulates both the plasticity and the output of the rat hippocampal formation. Bursts of TA activity can, depending on their timing, either increase or decrease the probability of Schaffer-collateral (SC)-evoked CA1 spikes. TA bursts can also significantly reduce the magnitude of synaptic potentiation at SC–CA1 synapses. The TA–CA1 synapse itself exhibits both long-term depression (LTD) and long-term potentiation (LTP). This capacity for bi-directional plasticity can, in turn, regulate the TA modulation of CA1 activity: LTP or LTD of the TA pathway either enhances or diminishes the gating of CA1 spikes and plasticity inhibition, respectively.

Using hippocampal slices optimized for stimulating both the SC and TA inputs[7,8] (Fig. 1a, b), we examined whether TA activity can gate SC-elicited spikes in CA1 pyramidal neurons. We first began with an SC stimulus strength that consistently evoked an excitatory postsynaptic potential (EPSP) but never a spike (Fig. 1c). We found that when the SC stimulus was immediately preceded by a TA burst (10 stimuli at 100 Hz), the previously ineffective SC stimulus now evoked a spike. The spike enhancement occurred when the TA stimulus preceded the SC stimulus by 20–80 ms, suggesting temporal summation of the TA- and SC-elicited EPSPs (Fig. 1c, d). The opposite phenomenon, spike-blocking[8,9], can also be observed. In this case, the SC axons are stimulated at a strength that reliably elicits a CA1 spike. If a short burst is delivered to TA axons about 400 ms before the SC stimulus, SC-elicited spiking of CA1 neurons is prevented (Fig. 1e). This is due to a $GABA_B$ (γ-aminobutyric acid)-mediated IPSP that reduces postsynaptic excitability; this IPSP can last for up to 1 s after a TA burst[8]. These data show that, depending on the relative timing of the TA input and the strength of SC stimulation, TA activity can either facilitate or block CA1 output. When a burst of TA activity precedes SC activity by $\leq$100 ms, SC-elicited spiking will tend to be facilitated. Conversely, TA activity that precedes SC activity by as much as 200 ms will tend to inhibit SC-elicited spiking. Because CA1 neuron activity constitutes the principal output of the hippocampal formation, these data suggest that TA activity can gate information transfer out of the hippocampus.

The capacity for TA activation to influence SC-driven spiking suggests that TA activity might also modulate plasticity at the SC–CA synapses. Indeed an earlier study indicated that stimulation of the TA pathway could reduce LTP at the SC–CA1 synapses[10]. We re-examined this issue in the following way: we first determined a SC theta burst stimulation (TBS) protocol that could be applied repeatedly, each time yielding roughly the same magnitude and pattern of synaptic potentiation (Fig. 2a, d). We then examined the

effects of TA activity on SC plasticity by jointly stimulating the two pathways. We used a TBS protocol to stimulate the TA path, as this most closely resembles the firing pattern of layer III entorhinal cortical neurons recorded *in vivo*[11,12]. We found that simultaneous stimulation of the TA and SC fibres (the onset of TA TBS preceded SC TBS by 20 ms) significantly reduced the both the magnitude and the duration of SC plasticity (Fig. 2b–d). After the joint TA + SC stimulation, significantly greater plasticity was consistently elicited by a subsequent SC-alone theta burst episode (Fig. 2b–d). In addition to diminishing the magnitude of the plasticity, joint TA + SC stimulation resulted in an earlier return to baseline levels of synaptic transmission, when compared with plasticity elicited by SC stimulation alone (Fig 2a–c). TA-induced inhibition of SC plasticity requires $GABA_A$-mediated transmission, as bicuculline (20 μM) completely prevented the plasticity interference usually imposed by joint stimulation (Fig. 2d). Indeed, in the presence of bicuculline a TA-induced enhancement of plasticity was observed, indicating that, in the absence of synaptic inhibition, TA-evoked EPSPs can sum, thereby facilitating SC–CA1 plasticity. Together with a previous study[10], these data demonstrate that the TA pathway can regulate the plasticity of the SC–CA1 synapse.

The gating of spikes and plasticity indicates that the TA pathway can modulate the activity of the trisynaptic circuit. However, it is also possible that the TA input provides 'information' as well as modulation to the hippocampus. If this is so, the capacity for plasticity of TA transmission is probably important. Although LTD of TA synaptic transmission has been observed[7], LTP has not been observed in hippocampal slices unless synaptic inhibition is prevented. We therefore re-examined the ability of the TA–CA1 synapses to exhibit LTP. We simultaneously recorded the SC- and TA-evoked field excitatory responses in stratum radiatum (SR) and stratum lacunosum moleculare (SLM), respectively, under conditions in which synaptic inhibition was intact. Four trains of high-frequency stimulation (HFS) to the TA axons resulted in a robust and long-lasting potentiation of synaptic transmission (Fig. 3a) (mean percentage of baseline at 60 min after tetanus, 136.1 ± 2.9%; $n = 25$). The simultaneously recorded SC–CA1 response did not change upon induction of TA-LTP, providing further evidence that we obtained a complete separation of the two inputs (Fig. 3a) ($n = 25$). Consistent with the presence of NMDA (*N*-methyl-D-aspartate) receptors in SLM dendrites[13] was the observation that this TA–CA1 potentiation was blocked by an NMDA-receptor antagonist, D-2-amino-5-phosphonopentanoate (AP5) (50 μM), present during the tetanus (Fig. 3b) ($n = 7$). Thus, TA–CA1 synapses exhibit both long-lasting depression[7] and potentiation, indicating that these synapses are capable of bidirectional synaptic modifications.

TA synaptic transmission can modulate both SC–CA1 spike activity and synaptic plasticity, and is itself subject to either upmodulation or downmodulation by LTP and LTD, respectively. Given these properties, we next examined whether the modulation of SC synaptic transmission by TA is plastic, in other words whether the TA-induced modulation of SC spikes or plasticity can be increased or decreased by LTP or LTD of the TA pathway. We addressed this in the following manner: we obtained baseline measurements of spike blocking or spike enhancement; we then induced either LTP or LTD in the TA pathway, and lastly we reassessed the efficacy of spike blocking or spike enhancement. As shown in Fig. 4, the induction of TA plasticity had a potent effect on

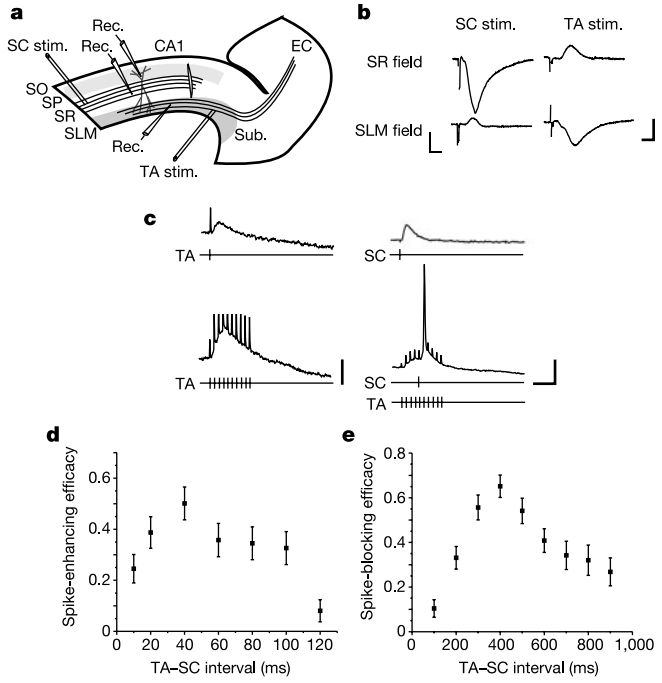

Figure 1 Enhancement and inhibition of SC-driven spikes by stimulation of TA. **a**, Recording set-up: two stimulating electrodes are used, one each in the SC and the TA. Extracellular recordings are made in SR and/or SLM. An intracellular recording from a CA1 neuron records responses elicited both in SC and in TA. **b**, Isolation of SC and TA field potentials. Stimulation of the SC results in a negative-going (sink) field potential recorded in SR and a positive-going (source) field potential in SLM. The converse is observed with TA stimulation. Scale bars, 0.5 mV (vertical), 5 ms (horizontal). **c**, Representative intracellular responses to either a single stimuli or a burst delivered to the TA or SC. When a single SC stimulus is presented alone no CA1 spike is elicited; when the SC stimulus is preceded by a TA burst that begins ~20 ms before the SC stimulus a spike is elicited. Scale bar, 5 mV (TA, vertical) or 20 mV (SC, horizontal), 50 ms. **d**, Spike enhancement as a function of the time by which the TA burst precedes the single SC stimulus ($n = 21$). **e**, Spike blocking as a function of TA–SC offset ($n = 32$).

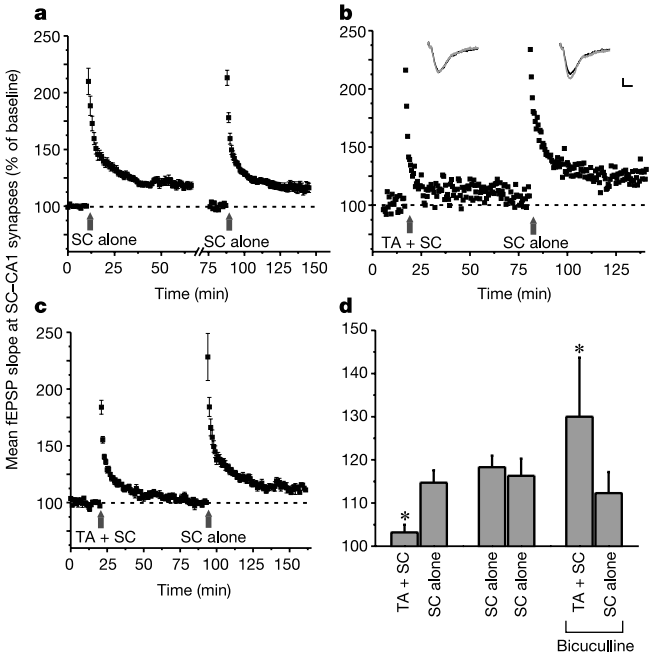

Figure 2 Interference with plasticity by stimulation of TA. **a**, Ensemble of experiments in which two consecutive epochs of TBS were delivered to the SC, each resulting in a comparable amount of potentiation (see also **d**) ($n = 12$). Dashed line, baseline synaptic transmission. **b**, When the SC TBS is coupled with TA stimulation, SC–CA1 plasticity is inhibited. Scale bars, 0.25 mV (vertical), 10 ms (horizontal). Traces are SC field before (solid) and after (dashed) stimulation. **c**, Ensemble of all plasticity interference experiments ($n = 8$). **d**, Mean SC–CA1 fEPSP potentiation, 50–60 min after stimulation. Potentiation of TA + SC was significantly lower than potentiation of SC alone. Bicuculline prevented plasticity interference and resulted in facilitation ($n = 6$).

the CA1 spike gating. To avoid ceiling or floor effects, the initial magnitude of either spike enhancement or blocking determined whether TA-LTP or TA-LTD would be subsequently induced. In experiments in which little spike enhancement was initially observed, the induction of TA-LTP greatly facilitated spike enhancement (Fig. 4a, b). Conversely, when strong spike enhancement was initially observed, its magnitude was markedly reduced by the induction of LTD at TA–CA1 synapses (Fig. 4c, d). The spike blocking phenomenon was also potently modulated by TA plasticity. In experiments in which low levels of spike blocking were initially observed, TA-LTP facilitated subsequent spike-blocking attempts (Fig. 4e, f). Conversely, after TA-LTD the spike-blocking efficacy was reduced (Fig. 4g, h). Thus, the effect of TA plasticity was either to increase or to decrease the gain of spike gating: LTP increased the magnitude of both spike enhancement and blocking, whereas LTD decreased both phenomena.

We next determined whether plasticity in the TA pathway also changes its ability to modulate SC–CA plasticity. We assessed the potency of plasticity interference before or after establishing TA plasticity. As before, the initial level of plasticity interference dictated whether TA-LTP or LTD would be induced: high initial levels of plasticity interference were usually followed by LTD induction, whereas low levels were usually followed by LTP induction. The induction of LTP at TA synapses consistently increased the magnitude of plasticity interference (Fig. 5a, b); joint TBS of the TA and SC pathway resulted in smaller amounts of potentiation at the SC–CA1 synapses after TA-LTP (see Supplementary Information for simultaneously recorded TA responses). Thus, LTP induction at the TA synapses increased its ability to interfere with SC–CA1 plasticity. The opposite was true of LTD induction: interference with plasticity was reduced. The magnitude of SC–CA1 potentiation observed after TA-LTD was greater, indicating that the modulatory capabilities of the TA pathway were reduced (Fig. 5c, d). A change in the degree of plasticity interference was observed only when TA plasticity was induced; in separate experiments we examined the stability of plasticity interference by repeatedly testing the magnitude of potentiation observed after joint TA + SC stimulation. When plasticity interference was initially low it stayed low in the absence of plasticity (Fig. 5b); conversely, when plasticity interference was initially high it stayed high in the absence of TA plasticity (Fig. 5d). Thus, like the spike gating imposed by TA activity, the plasticity interference is also subject to significant modulation by plasticity of the TA–CA1 synapses themselves.

Thus, our data show that the TA–CA1 synapses can be either potentiated or depressed; this modification of the TA synapses by plasticity in turn modulates this pathway's ability to gate the output or plasticity of SC–CA1 synapses. Modulation of excitatory synaptic connections on inhibitory interneurons whose processes extend into SLM also influences the strength of TA–CA1 activity[8,14]. The results indicate that the net TA modulation of CA3–CA1 synaptic transmission will be influenced dynamically by both the strength of the TA–CA1 synaptic connections as well as the relative timing of the TA and trisynaptic inputs to CA1. Detailed knowledge of the temporal firing properties of the different entorhinal cortical layers is needed for a full understanding of the interplay between these two inputs to CA1 pyramidal neurons.

These results indicate an important modulatory role for the TA pathway but also raise the possibility of a more fundamental role of TA–CA1 synaptic transmission in hippocampal information processing. The hippocampal formation is firmly established as being necessary for the formation and retention of declarative memories. In characterizing the synaptic contributions that underlie hippocampus-dependent memories, most studies have focused on entorhinal input to the dentate gyrus that is then serially processed

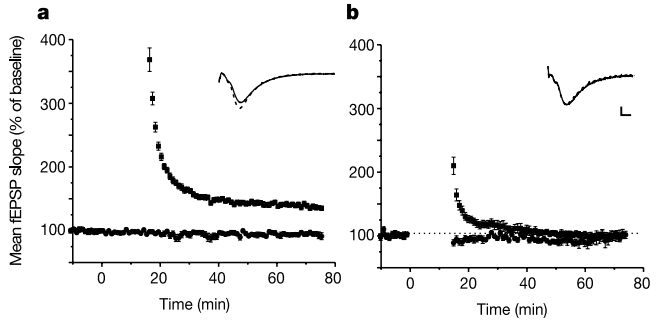

Figure 3 TA–CA1 synapses exhibit NMDA-receptor-dependent LTP. **a**, Ensemble of all TA LTP experiments. HFS resulted in significant potentiation of TA–CA1 synaptic transmission (squares) without affecting the SC–CA1 synaptic responses (circles) recorded simultaneously. **b**, Ensemble of all TA-LTP experiments conducted in the presence of an NMDA-receptor antagonist, AP5. Scale bars in insets, 0.1 mV (vertical), 10 ms (horizontal).

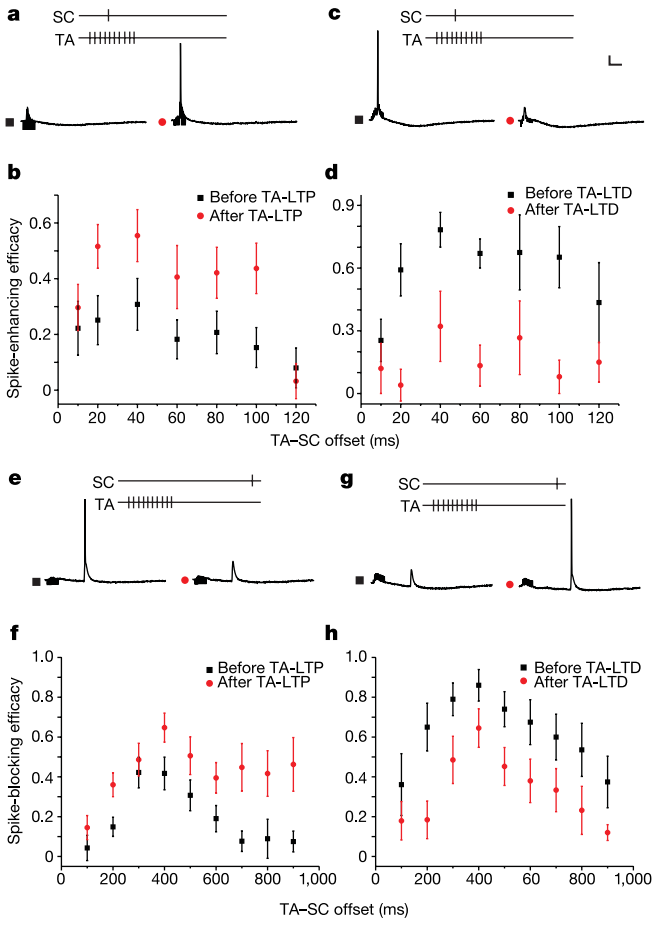

Figure 4 Modulation of spike blocking and spike enhancement by TA-LTP and LTD. **a**, Spike-enhancement protocol and CA1 neuron intracellular record before (black square) and after (red circle) TA-LTP. **b**, Summary of spike enhancement (TA–SC offset is the time by which the TA burst precedes the SC stimulus) before and after TA-LTP ($n = 15$). **c**, Spike enhancement protocol and CA1 neuron intracellular record before (black square) and after (red circle) TA-LTD. **d**, Analysis of all experiments showing the amount of spike enhancement achieved before and after TA-LTD ($n = 6$). **e**, Spike-blocking protocol and CA1 neuron record before (black square) and after (red circle) TA-LTP. **f**, Summary data showing spike blocking before and after TA-LTP ($n = 22$). **g**, Spike-blocking protocol and CA1 neuron record before (black square) and after (red circle) TA-LTD. **h**, Summary of spike blocking before and after TA-LTD ($n = 10$). Scale bars for **a**, **c**, **e**, **g**: 10 mV (vertical), 100 ms (horizontal).

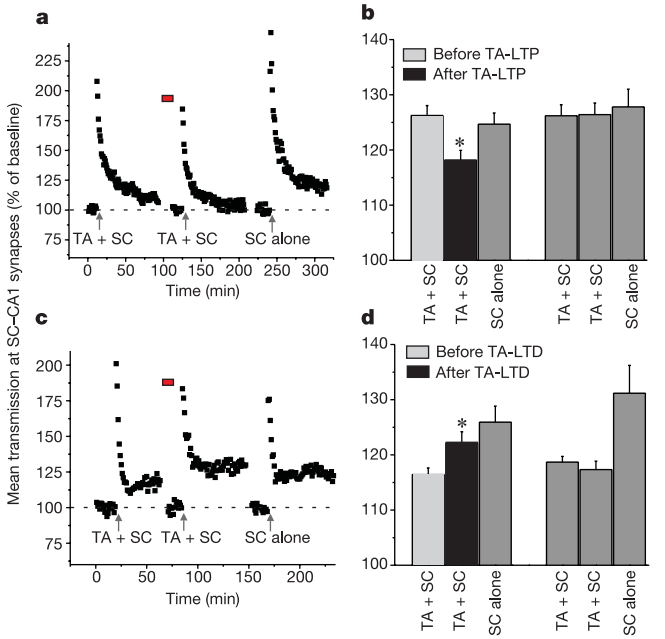

Figure 5 Modulation of interference with plasticity by TA-LTP and LTD. **a**, Representative experiment monitoring SC–CA1 transmission in which LTP in the TA pathway (at the time indicated by the red-filled oblong) increased the plasticity interference. **b**, Summary of the potentiation for each TA + SC stimulation epoch (first two bars) before and after LTP and the enhancement observed after SC stimulation alone. TA-LTP significantly increased plasticity interference ($n = 24$). In separate control experiments (right bars), no change in plasticity interference occurred when the TA + SC stimulation was applied again ($n = 5$). **c**, Representative experiment in which TA-LTD (at the time indicated by the red-filled oblong) decreased plasticity interference. **d**, Summary of the potentiation for each TA + SC stimulation epoch before and after TA-LTD and the enhancement observed after SC stimulation alone. TA-LTD significantly decreased plasticity interference ($n = 11$). In separate control experiments no change in plasticity interference occurred when TA + SC stimulation was applied again ($n = 5$).

by synapses in areas CA3 and CA1 (the trisynaptic circuit). However, some studies suggest that the trisynaptic circuit is not necessary for some kinds of spatial memory[15,16]. A distinguishing feature of pyramidal neurons of area CA3 or CA1 is their firing selectivity for particular locations in the animal's environment, the so-called 'place fields'[17]. These place fields are thought to contribute to hippocampus-dependent spatial behaviours. Some studies have shown that the trisynaptic circuit is not required for the establishment of place-selective cells[18,19]. In these studies, the ablation of dentate granule cells[18] or CA3 pyramidal neurons[19] does not abolish CA1 place fields. Our plasticity results suggest that, in addition to modulating trisynaptic hippocampal function, the TA pathway could provide the information required for important aspects of memory and place-cell function. □

Methods

Slice preparation and electrophysiology

Slices were prepared and microdissected to isolate the TA pathway, as described previously[7,8]. In brief, after decapitation and removal of the brain, the dorsal surface of the posterior half of each hemisphere was glued to the stage of a cooled oscillating tissue slicer and covered with chilled artificial cerebrospinal fluid (ACSF) containing (in mM) 119 NaCl, 2.5 KCl, 1.3 $MgSO_4$, 2.4 CaCl, 1.0 NaH_2PO_4, 26.3 $NaHCO_3$, 11.0 glucose. Slices (500 μM) were cut, with the optimal slices (as assessed visually, by ease of identification of distinct layers, as well as electrophysiologically, by the presence of robust field potentials) generally found 4–4.5 mm below the ventral surface. Bipolar tungsten electrodes, either concentric or paired needles, were used for stimulation. One electrode was placed in SR to stimulate the SCs; the other in SLM to stimulate the TA pathway. Unless otherwise noted, all experiments were conducted with synaptic inhibition intact. Field recordings were made with low-resistance micropipettes filled with 3 M NaCl. The SC response was recorded in SR and the TA response in SLM. To clearly isolate the TA response it was necessary to dissect the slice further[7,8]. The entire dentate gyrus was removed to eliminate the possibility of activation of the trisynaptic pathway and to prevent the contamination of a field response recorded in SLM by the much larger field elicited in the dentate gyrus by concurrent activation of the perforant path. In most experiments CA3 was also removed to eliminate the possibility of disynaptic activation via the perforant path projection to CA3. In addition, a cut was made through SR in distal CA1 (near the subiculum) perpendicular to the cell body layer to prevent the antidromic activation of SC by the stimulation electrode in SLM. SCs do not enter SLM to any appreciable extent[4], so this cut cleanly isolates TA axons. Separation of the two pathways was confirmed by the observation of a positive-going field potential in the other layer[13]. Intracellular recording was conducted as described previously[7,8]. The following stimulation protocols were used: HFS, 100 Hz for 1 s, repeated 4 times at 5-min intervals; TBS, 8 bursts of either 5 (SC) or 10 (TA) pulses at 100 Hz, 200 ms between bursts; low-frequency stimulation (LFS), stimulation at 1 Hz for 10 min. All stimulus pulses were of the same length and amplitude as test pulses. Test pulses were applied once every 30 s to each pathway. The initial slope of the field EPSP was measured. Drugs were applied by dilution of concentrated stock solutions into the perfusion medium. All chemicals were obtained from Sigma (St Louis, Missouri).

Data analysis

Data were collected directly by an IBM-compatible computer using in-house software. All numerical values are listed as means ± s.e.m. unless otherwise stated. Depression and potentiation were measured by taking an average of the initial slopes of the field EPSPs (fEPSPs) over a 10-min period before and after the end of LFS, HFS or TBS. Spike-enhancing efficacy was calculated by measuring the spike probability (p) as follows: $[p(\mathrm{TA} + \mathrm{SC}) - p(\mathrm{SC\ alone})]/[1 + p(\mathrm{SC\ alone})]$.

Spike-blocking efficacy was calculated by measuring the spike probability (p) as follows: $[p(\mathrm{SC\ alone}) - p(\mathrm{TA} + \mathrm{SC})]/p(\mathrm{SC\ alone})$. Student's paired t-test was used to determine statistical significance for within-group comparisons; the unpaired t-test was used between groups. Data reported as significant (indicated by an asterisk in figures) achieved at least the $P \leq 0.01$ level. Points in figures represent means ± s.e.m. across all experiments. Representative traces, shown in insets, are averages of five consecutive sweeps from a representative experiment, taken 5 min before LFS, HFS or TBS, and 60 min after the end of LFS, HFS or TBS.

Received 26 December 2001; accepted 28 January 2002.

1. Morris, R. G. M., Garrud, P., Rawlins, J. N. P. & O'Keefe, J. Place navigation impaired in rats with hippocampal lesions. *Nature* **297,** 681–683 (1982).
2. Eichenbaum, H. A cortical–hippocampal system for declarative memory. *Nature Rev. Neurosci.* **1,** 41–50 (2001).
3. Witter, M. P., Groenewegen, H. J., Silva, F. H. L. D. & Lohman, A. H. Functional organization of the extrinsic and intrinsic circuitry of the parahippocampal region. *Prog. Neurobiol.* **33,** 161–253 (1989).
4. Amaral, D. G. & Witter, M. P. The three-dimensional organisation of the hippocampus: a review of the anatomical data. *Neuroscience* **31,** 571–591 (1989).
5. Cajal, S. R. *The Structure of Ammon's Horn* (ed. Thomas, C. C.) (Thomas, Springfield, Illinois, 1968).
6. Steward, O. & Scoville, S. A. Cells of origin of entorhinal cortical affferents to the hippocampus and fascia dentate of the rat. *J. Comp. Neurol.* **169,** 347–370 (1976).
7. Dvorak-Carbone, H. & Schuman, E. M. Long-term depression of temporoammonic-CA1 hippocampal synaptic transmission. *J. Neurophysiol.* **81,** 1036–1044 (1999).
8. Dvorak-Carbone, H. & Schuman, E. M. Patterned activity in stratum lacunosum moleculare inhibits CA1 pyramidal neuron firing. *J. Neurophysiol.* **82,** 3213–3222 (1999).
9. Empson, R. M. & Heineman, U. The perforant path projection to hippocampal area CA1 in the rat hippocampal–entorhinal cortex combined slice. *J. Physiol. (Lond.)* **484,** 707–720 (1995).
10. Levy, W. B., Desmond, N. L. & Zhang, D. X. Perforant path activation modulates the induction of long-term potentiation of the Schaffer collateral–hippocampal CA1 response: theoretical and experimental analyses. *Learn. Mem.* **4,** 510–518 (1998).
11. Chrobak, J. J. & Buzsaki, G. Gamma oscillations in the entorhinal cortex of the freely behaving rat. *J. Neurosci.* **18,** 388–398 (1998).
12. Chrobak, J. J., Lorincz, A. & Buzsaki, G. Physiological patterns in the hippocampo-entorhinal cortex system. *Hippocampus* **10,** 457–465 (2000).
13. Colbert, C. M. & Levy, W. B. Electrophysiological and pharmacological characterization of perforant path synapses in CA1: mediation by glutamate receptors. *J. Neurophysiol.* **68,** 1–8 (1992).
14. Maccaferri, G. & McBain, C. J. Passive propagation of LTD to stratum oriens-alveus inhibitory neurons modulates the temporoammonic input to the hippocampal CA1 region. *Neuron* **15,** 137–145 (1995).
15. Jarrard, L. E., Okaichi, H., Steward, O. & Goldschmidt, R. B. On the role of hippocampal connections in the performance of place and cue tasks: comparisons with damage to hippocampus. *Behav. Neurosci.* **98,** 946–954 (1984).
16. Jarrard, L. E. What does the hippocampus really do? *Behav. Brain. Res.* **71,** 1–10 (1995).
17. Muller, R. A quarter of a century of place cells. *Neuron* **17,** 813–822 (1996).
18. McNaughton, B. L., Barnes, C. A., Meltzer, J. & Sutherland, R. J. Hippocampal granule cells are necessary for normal spatial learning but not for spatially-selective pyramidal cell discharge. *Exp. Brain. Res.* **76,** 485–496 (1989).
19. Brun, V. H., Otnæss, M. K., Witter, M. P., Moser, M. B. & Moser, E. I. Place representation in hippocampal area CA1 in the absence of input from area CA3. *Soc. Neurosci. Abstr.* 31 (2001).

Supplementary Information accompanies the paper on *Nature's* website (http://www.nature.com).

Acknowledgements

We thank G. Laurent for critial reading of the manuscript. This work was supported by Fundacao para a Ciencia e Tecnologia (FCT)—Portugal and the Howard Hughes Medical Institute.

Competing interests statement

The authors declare that they have no competing financial interests.

Correspondence and requests for materials should be addressed to E.M.S. (e-mail: schumane@its.caltech.edu).

Pseudomonas biofilm formation and antibiotic resistance are linked to phenotypic variation

Eliana Drenkard & Frederick M. Ausubel

Department of Genetics, Harvard Medical School and Department of Molecular Biology, Massachusetts General Hospital, Boston, Massachusetts 02114, USA

Colonization of the lungs of cystic fibrosis (CF) patients by the opportunistic bacterial pathogen *Pseudomonas aeruginosa* is the principal cause of mortality in CF populations[1,2]. *Pseudomonas aeruginosa* infections generally persist despite the use of long-term antibiotic therapy[1,3]. This has been explained by postulating that *P. aeruginosa* forms an antibiotic-resistant biofilm[4,5] consisting of bacterial communities embedded in an exopolysaccharide matrix. Alternatively, it has been proposed that resistant *P. aeruginosa* variants may be selected in the CF respiratory tract by antimicrobial therapy itself[1,6]. Here we report that both explanations are correct, and are interrelated. We found that antibiotic-resistant phenotypic variants of *P. aeruginosa* with enhanced ability to form biofilms arise at high frequency both *in vitro* and in the lungs of CF patients. We also identified a regulatory protein (PvrR) that controls the conversion between antibiotic-resistant and antibiotic-susceptible forms. Compounds that affect PvrR function could have an important role in the treatment of CF infections.

Antibiotic-resistant colonies of *P. aeruginosa* clinical isolate PA14 (ref. 7) arose at a frequency of 10^{-6} to 10^{-7} when cultures were plated on Luria-Bertani (LB) agar containing kanamycin (200 $\mu g\,ml^{-1}$). Resistant colonies were smaller than wild-type even on antibiotic-free media, and exhibited colony morphologies similar to the ones described for CF variant isolates[6,8]. One class of the resistant variants (approximately 30%) exhibited a rough colony phenotype compared with the wild type, and was called RSCV (rough small-colony variant). When RSCVs were grown on antibiotic-free LB agar, wild-type revertants, characterized by a large colony size, smooth appearance, and wild-type levels of susceptibility to kanamycin, arose on the edges of the variant colonies after five days incubation at room temperature (Fig. 1a), suggesting that the phenotypic changes observed in the resistant variants were transient. In addition to being resistant to kanamycin, (40 times the wild-type susceptibility level), individual RSCV colonies were also resistant to amikacin (30 $\mu g\,ml^{-1}$), carbenicillin (300 $\mu g\,ml^{-1}$), gentamicin (30 $\mu g\,ml^{-1}$), tobramycin (10 $\mu g\,ml^{-1}$) and tetracycline (150 $\mu g\,ml^{-1}$). Consistent with this latter result, resistant variants were also obtained at frequencies of about 10^{-7} by plating cultures of PA14 on media containing similar concentrations of the antibiotics mentioned above.

Although RSCV colonies were smaller than wild type, their small colony size was not a consequence of slow growth, as the generation time of RSCV in liquid medium was not significantly different from that of the wild type, even in LB agar containing 200 $\mu g\,ml^{-1}$ kanamycin. Unlike the wild type, RSCV formed visible aggregates when liquid cultures were left without shaking at room temperature (Fig. 1b). Moreover, RSCVs exhibited increased attachment to glass (not shown) and polyvinylchloride plastic (PVC) (Fig. 1c). Reverted RSCV showed wild-type levels of both agglutination and attachment to glass and PVC plastic (data not shown).

Because the ability of bacteria to attach to each other and to surfaces depends in part on the interaction of hydrophobic domains[9], we determined the surface hydrophobicity of RSCV relative to the wild type. RSCV clones agglutinated at a lower salt concentration (0.125 M) than wild-type PA14 (0.5 M), indicating that RSCVs had a higher degree of surface hydrophobicity. Similarly, 200 mM tetramethyl urea (TMU), a hydrophobic bond-breaking agent, reduced the attachment of RSCV cells to PVC plates to wild-type levels (data not shown). Several RSCV clones were tested in the experiments described above, and all exhibited similar phenotypes. A single RSCV clone, referred to as RSCV for simplicity, was therefore chosen for further analysis.

Recently, it has been shown that *P. aeruginosa* in the sputum of CF patients exists primarily as a biofilm[4]. To determine whether the antibiotic-resistant phenotype of RSCV is associated with altered biofilm formation, biofilms of PA14 or RSCV expressing green fluorescent protein (GFP) were cultivated in flow chambers under continuous culture conditions. Analysis of biofilm structures using confocal scanning laser microscopy (CSLM) showed that RSCV formed biofilm faster (RSCV microcolonies appeared 4–5 h earlier

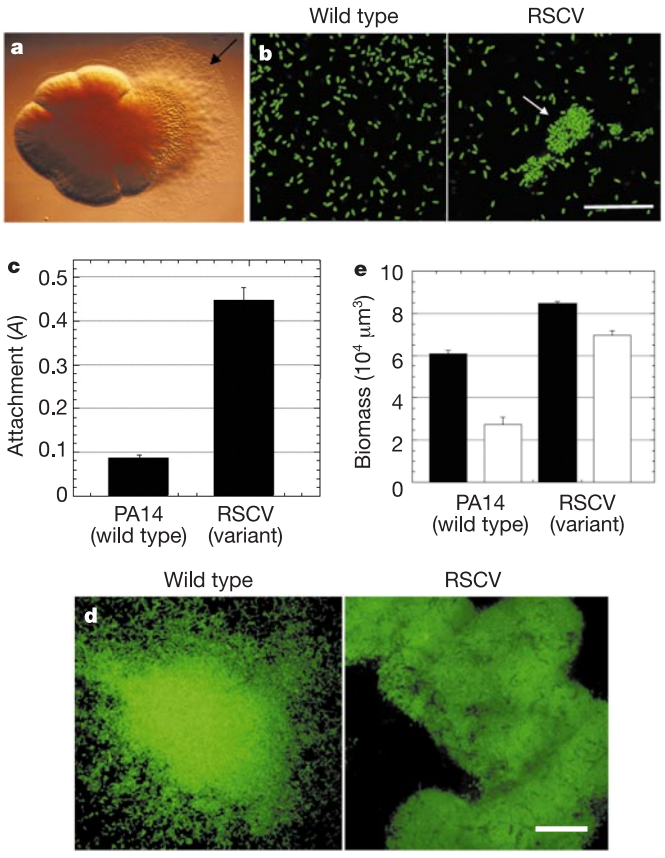

Figure 1 Characterization of *P. aeruginosa* antibiotic-resistant RSCV. **a**, Reversion of RSCV was observed on the edges of colonies (arrow) on antibiotic-free media, 30 × . **b**, CSLM analysis of bacterial aggregates (arrows) expressing GFP after growth in liquid broth. Scale bar, 25 μm. **c**, Attachment of wild-type PA14 and RSCV to PVC (see Methods). *A*, absorbance. **d**, CSLM analysis of biofilm formed by wild-type PA14 and RSCV expressing GFP. Scale bar, 50 μm. **e**, Resistance of biofilms to tobramycin was determined by measuring viable biomass on 45-h-old established biofilms before (filled bars) and after (open bars) 36-h tobramycin (200 $\mu g\,ml^{-1}$) treatment. In the absence of antibiotic treatment, both PA14 and RSCV biofilms grew at constant rates (not shown).